Geosynthetics anchorage with wrap around: experimental and numerical studies

S. H. Lajevardi[1], C. Silvani[2], D. Dias[3], L. Briançon[4] and P. Villard[5]

[1]*Associate Professor, Islamic Azad University, Arak Branch, Iran, Telephone: +98 (0) 9128521975; Telefax: +98 (0) 2532615943; E-mail: Hamidlajevardi@yahoo.com*
[2]*Associate Professor, INSA de Lyon, LGCIE, Villeurbanne, France, Telephone: +33 (0) 4 72 43 83 69; Telefax: +33 (0) 4 72 43 85 21; E-mail: claire.silvani@insa-lyon.fr*
[3]*Professor, Grenoble Alpes University, 3SR, Grenoble, France, Telephone: +33 (0) 4 76 82 79 31; Telefax: +33 (0) 4 76 82 79 01; E-mail: Daniel.dias@ujf-grenoble.fr (corresponding author)*
[4]*Associate Professor, INSA de Lyon, LGCIE, Villeurbanne, France, Telephone: +33 (0) 4 72 43 83 70; Telefax: +33 (0) 4 72 43 85 20; E-mail: laurent.briancon@insa-lyon.fr*
[5]*Professor, Grenoble Alpes University, 3SR, Grenoble, France, Télephone: +33 4 56 52 86 28; Telefax: +33 4 76 82 70 43; E-mail: Pascal.Villard@ujf-grenoble.fr*

Received 06 February 2014, revised 15 November 2014, accepted 07 March 2015

ABSTRACT: Geosynthetics are used as reinforcing elements in a wide variety of structures: reinforced slopes and walls; embankments on soft soils; piled embankment; reinforcement in the base layers of railroad and road constructions; reinforced foundation mattresses; bridging of sinkholes or reinforced abutments. In some cases, these reinforced structures require anchorage areas. Designing the required dimensions of this anchorage remains problematic. This paper focuses on the simple run-out and wrap around anchorages. Laboratory tests, performed with these two anchorage benches, consisted of the pull-out of three geotextiles (uniaxial or biaxial with different stiffness) anchored following various geometries in different kinds of soil. In order to confirm and to complete the experimental studies presented in these anchorage systems, a specific two-dimensional discrete-element model has been used. The soil was described by discrete elements and the geosynthetic behaviour was taken into account by the use of thin finite elements. The interface behaviour between the soil particles and the geosynthetic elements was considered at each contact point by using a Coulomb contact law. The numerical model reproduced the experimental campaign and the anchorage mechanisms reasonably. The load transfer between the geosynthetic and soil was visualised by the force and displacements distribution along the geosynthetic sheet. The numerical procedure could also be used to define the conditions of stability for reinforced slopes or walls.

KEYWORDS: Geosynthetics, Anchorage systems, Pull-out test, Soil reinforcement, Discrete element model

REFERENCE: Lajevardi, S. H., Silvani, C., Dias, D., Briançon, L. and Villard, P. (2015). Geosynthetics anchorage with wrap around: experimental and numerical studies. *Geosynthetics International*, **22**, No. 4, 273–287. [http://dx.doi.org/10.1680/gein.15.00010]

1. INTRODUCTION

The stability and durability of geosynthetics in reinforced earth structure depends partly on the efficiency of the anchors holding the geosynthetic sheets. Wrap around anchorages are used generally inside reinforced slopes or walls. The role of the anchor is to withstand the tension generated in geosynthetic sheets by the structure. Designing the required dimensions of this anchorage remains problematic. Several authors studied the behaviour of these anchorage systems numerically and experimentally. They showed that the pull-out test is the most suitable test to determine the soil/geosynthetic interface under low and high confinement stress and to support numerical studies in order to determine the behaviour and the anchorage capacity (Chareyre *et al.* 2002; Gourc *et al.* 2004; Chareyre and Villard 2005; De and Vellon 2005; Girard *et al.* 2006; Briançon *et al.* 2008; Su *et al.* 2008; Khedkar and Mandal 2009; Palmeira 2009; Sieira *et al.* 2009; Abdelouhab *et al.* 2010; Lajevardi *et al.* 2013, 2014, 2015). The soil–geosynthetic interaction can be complex because it is affected by structural, geometrical and mechanical characteristics of the geosynthetic, as well as by boundaries and loading conditions (Moraci and Recalcati 2006; Calvarano *et al.* 2013; Cazzuffi *et al.* 2014; Moraci *et al.* 2014) and the mechanical properties of soil.

An alternative approach investigating the behaviour of reinforced earth structures is to use numerical simulations. The finite-element method (FEM) is one of the most widely used numerical simulation techniques in geotechnical engineering, but it has limitations for some applications and it could not provide insight into kinematic behaviour of discontinuous media at a microscopic level. The discrete-element method (DEM) is an alternative numerical simulation technique, which assumes that the model is composed of particulate matters (Zhang *et al*. 2013) has been successfully used by many researchers to study the geosynthetic-reinforced soil and embankment behaviour (Chareyre *et al*. 2002; Villard and Chareyre 2004; Chareyre and Villard 2005). Many researchers have modelled soil/geosynthetic interaction by DEM to understand the behaviour of granular materials (sand or ballast) under complex loading conditions. Using DEM, some researchers studied the interlocking effect between soil and geogrid to understand mechanisms for soil stabilisation (Ferellec and McDowell 2012; Stahl *et al*. 2014) and investigate load transfer behaviour between the geosynthetic and the soil (Ferellec and McDowell 2012; Chen *et al*. 2012; Han *et al*. 2012; Wang *et al*. 2014). The capacity of anchorage in pull-out tests has been widely studied either on geogrids (McDowell *et al*. 2006; Zhang *et al*. 2007) or on geotextile anchorages (Briançon *et al*. 2008). More complex loading conditions or soil reinforcement have been simulated using DEM: Bhandari and Han (2010) investigated the interaction between a geotextile and soil under a cyclic vertical load, and Chen *et al.* (2012) studied the cyclic loading of geogrid-reinforced ballast under confined or unconfined conditions. Lin *et al*. (2013) investigated a new type of soil reinforcement in geotechnical engineering: they carried out experimental and discrete element analysis on two layers horizontal–vertical reinforcing elements in triaxial compression tests, then (Zhang *et al*. 2013) studied the behaviour of soil embankments reinforced with these two layer inclusions. Han *et al.* (2012) conducted discrete element simulations of geogrid-reinforced embankments over piles.

Usually, in each approach mentioned identified earlier, the geosynthetic is modelled using a set of spherical particles bonded together. The interaction between the geosynthetic and the soil is defined through the contact points between discrete particles. Although microscopic parameters of the bonded geosynthetic particles used to model the geosynthetic are determined using index load tests. Moreover, as a set of bonded particles are used to consider the continuous nature of the geosynthetic, the complex geosynthetic deformation may not be accurately considered in a pull-out test due to the inflexibility of the bonded particles (Tran *et al*. 2013). Therefore, the strains and stresses within the geosynthetic may not be accurately obtained.

In order to solve this problem, the reinforcement layer can be modelled using the FEM whereas the backfill soil can be modelled using the DEM. The coupling of the two methods can efficiently model the behaviour of the geosynthetic as well as the backfill soil material. This approach has been used by several researchers in geosynthetic-reinforced earth structures (Chareyre and Villard, 2005; Villard *et al*. 2009; Tran *et al*. 2013).

This study focuses on the simple run-out and wrap around anchorages (the interest of the wrap around anchorage is to reduce the anchorage area). Two French research laboratories (Irstea and INSA Lyon) performed tests jointly with two anchorage benches on the same reinforced non-woven needle-punched geotextile and with the same geometry of anchorage in cohesive and non-cohesive soils. Laboratory tests performed with INSA anchorage apparatus (Lajevardi *et al*. 2014, 2015) are simulated with a two-dimensional DEM.

2. LABORATORY TESTS

The anchoring behaviour of a geosynthetic sheet under tension was studied experimentally with pull-out tests. The pull-out tests were carried out with an experimental device consistent with the standards recommendations in ASTM D6706-01 and BS EN 13738 (BSI, 2004). This physical model consisted of a 1 m wide and 2.50 m long bench for the Irstea anchorage apparatus (Figure 1a) and of a 1.00 m wide and 2.00 m long bench for the INSA anchorage apparatus (Figure 1b).

The traction system was fixed onto the geosynthetic (geotextile or geogrid) with a metallic clamp. The tensile force (applied on the geosynthetic sheet width), the

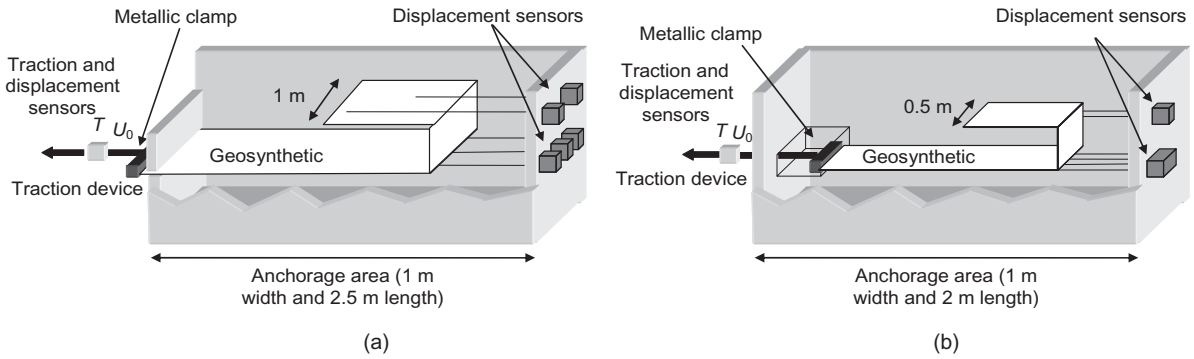

Figure 1. Anchorage benches: (a) Irstea bench, (b) INSA bench

displacements of the metallic clamp and the anchorage area were monitored during the pulling out test.

2.1. Anchorage benches

The Irstea anchorage apparatus (Figure 1a) included a 1 m wide anchor block and a traction device. This device was fixed onto the geotextile using a metallic clamp located outside the anchor block (supposed to be indeformable). The tension T (applied on the 1 m width geosynthetic sheet: $b = 1$ m) and the displacement U_0 of the tensile cable were monitored on pulling out using sensors fixed onto the tensile system. In the anchorage area, a cable measuring system was used to monitor the displacements of the geotextile at different points.

The INSA anchorage apparatus (Figure 1b) included 1 m wide anchor block and a traction device allowing the pull out of a 0.5 m width geosynthetic sheet ($b = 0.50$ m). This device was fixed onto the geotextile with a metallic clamp located in a box inside the anchor block (supposed to be indeformable). As for the first anchorage bench, the tension T, the displacement U_0 of the tensile cable and the geotextile displacement were monitored on pulling out using similar sensors.

The principal differences between both apparatus were the localisation of the metallic clamp sited between the geosynthetic and the tensile system, the width of the geosynthetic samples and pull-out rate.

2.2. Traction device

2.2.1. *INSA bench*

The traction device was conceived specifically for this pull-out test. The idea was to build a system that would be able to transmit the tensile force to the geosynthetic, such as

- the pressure was as homogeneous as possible over the width of the sheet
- there was no relative displacement of the reinforcement from the metallic clamp (no sliding).

The metallic clamp connected the reinforcement to the jack and distributed the tension efforts to the reinforcement equally (Figure 1b). In order to avoid the effects of the front wall (roughness and stiffness), the reinforcement was placed at a certain distance (0.50 m) from it using a guidance box (0.50 m × 0.70 m × 0.16 m) located inside the box. The metallic clamp was placed in this guidance box to prevent any contact with the soil that would lead to additional tensile efforts (Figure 1b).

2.2.2. *Irstea bench*

The traction device was located outside the bench. Reinforcement was installed on the flat surface of the soil and connected to an extraction jack positioned in front of the bench. In the traditional pull-out test, the soil was in contact with the rigid frontal face and the friction along this face must be minimised. On the Irstea bench, sleeves were used to reduce the friction.

2.3. Anchorage geometry

Several anchorage shapes have been used to highlight the mechanisms of interaction between soil and geosynthetic (Figure 2) and to determine the optimum anchorage according to the kind of soil and the geosynthetic characteristics. Simple run-out was specially performed to determine the friction angle between the soil and geotextile and to observe the friction mobilisation according to the anchorage length ($L = 1$ or 1.5 or 2 m). Various anchorages with wrap around were carried out to establish the influence of geometry on anchorage capacity.

- Thickness of soil layer above anchorage ($H = D_1 + D_2 = 0.36$, 0.4 or 0.5 m).
- Distance between upper and lower parts of geotextile ($D_1 = 0.2$ or 0.3 m).
- Length of upper part of sheet ($B = 0.25$, 0.5 or 1 m).
- $D_2 = 0.2$ m.
- Width of the geosynthetic sheet (anchorage width: $b = 0.5$ or 1 m).

2.4. Materials tested

Four soils were used for these tests: two sands, a sandy silt and a gravel. Their main properties were measured and they are presented in Table 1. Figure 3 presents the distribution curve of grain-size for the soils used in the study. The geosynthetics used for these tests were reinforcement geotextiles (uniaxial or biaxial) constituted by high modulus polyester wires, attached to a continuous filament nonwoven geotextile backing. According to their reinforcement level, three geosynthetics were tested (Table 2, Figure 4).

2.5. Sensors

2.5.1. *Displacement sensors*

Cable displacement sensors were used to measure displacements along and at the head of the geotextile sheet (Figure 5). They were placed on the support at the front and at the back of the tank then lengthened and connected by a steel cable at various points on the reinforcement. These sensors allowed measurement of the displacement of the metallic clamp (U_0) at the beginning, middle and end of the geotextile sheet (C1, C2 and C3).

2.5.2. *Traction (load) sensor*

In order to measure the tension, a load sensor was placed between the extraction jack and the connection system.

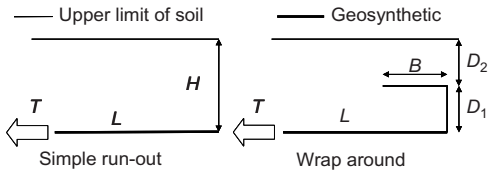

Figure 2. Anchorage geometry

Table 1. Soil properties

Soil	γ_d (kN/m^3)	w (%)	D_{10} (mm)	D_{30} (mm)	D_{60} (mm)	φ' (°)	c' (kPa)
Sand 1	15.2	1	0.22	0.3	0.42	35	1
Sand 2	20.0	5	0.15	0.3	0.5	37	4
Sandy silt	15.7	2.5	–	–	–	30	22
Gravel	19.5	1	0.5	2.3	9.5	37	8

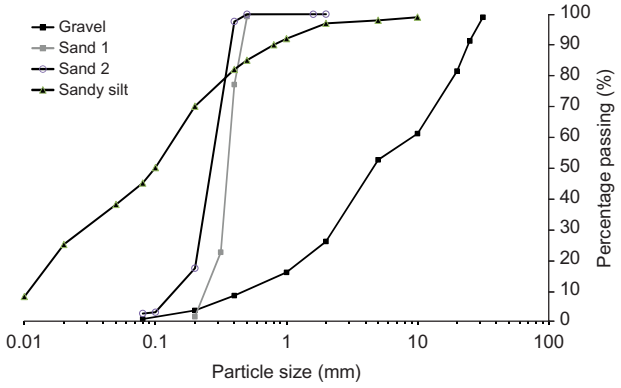

Figure 3. Distribution curves of grain-size for the soils used in the study

2.5.3. *Pressure sensor*
In the INSA anchorage bench and for the simple run-out anchorage, a total pressure sensor was installed, over the metallic clamp, at the front tank to measure the horizontal stress (Figure 5).

2.6. Procedure

2.6.1. *Initial phase*
The tests were carried out in the following way: A first layer of soil was laid out with an average 0.20 m thickness. The soil (gravel or sand) layer was evenly compacted with a rammer. The geotextile sheet was set up on the flat surface of the soil and connected to an extraction jack located in the front of the box. Displacement sensors located at the back of the box, were connected to many points along the reinforcement.

2.6.2. *Next phase for the simple run-out*
After connecting all the displacement sensors, a 0.40 or 0.50 m thick layer of soil (H) was laid out over the reinforcement. The soil was set up layer by layer (for $H = 0.40$ m: two successive layers, 0.20 m high and for $H = 0.50$ m: three successive layers, 0.20, 0.10 and 0.20 m high) and every layer was compacted with a rammer. Monitoring was performed at every new layer: for a given volume of soil its weight was measured. After the last compacted layer, the extraction jack was started. Within the framework of these tests, the pull-out rate was fixed at 1 mm/min (Alfaro *et al.* 1995; Abdelouhab *et al.* 2010; Lajevardi *et al.* 2013). The pull-out test was carried out and stopped as soon as the tension reached a plateau and all the displacement sensors monitored displacements. This double condition ensured that the friction was mobilised over the entire length of the reinforcement.

2.6.3. *Next phase for the wrap around anchorage*
Once the first reinforcement part (L) was placed and equipped with displacement sensors, the reinforcement was held vertically to a depth D_1. Soil layers were laid out above the horizontal reinforcement length (L) and were compacted uniformly with a rammer. If $D_1 = 0.20$ m, there was only a single layer and if $D_1 = 0.30$ m, there were two layers of 0.20 and 0.10 m. Once the height D_1 was reached, the reinforcement was folded over for a length of B. This part of reinforcement was also equipped with displacement sensors. One layer of soil was placed above the length of upper part of sheet ($D_2 = 0.20$ m). After the last compacted layer, the extraction jack was started with a rate of 1 mm/min. The pull-out was carried out and stopped using the same dual criteria as for the simple run-out.

3. EXPERIMENTAL TESTS RESULTS

3.1. Simple run-out anchorage

The pull-out mechanisms in both anchorage benches were compared in the case of simple run-out anchorage. For the Irstea bench (Figure 6), two inflection points were observed (three slopes) in the curve of the tension versus the head displacement (T–C1). The behaviour that was observed before the first point corresponded to the

Table 2. Geosynthetic properties

GSY		Stiffness: J (kN/m)	Thickness (mm)	Tensile strength MD (kN/m)		Unit weight (g/m²)
				At 2% strain	Ultimate	
GT_{75}	biaxial	687	2.6	16	79	440
GT_{95}	biaxial	870	3	20	100	540
GT_{230}	uniaxial	2104	3.2	46	242	620

GSY, geosynthetic; MD, machine direction.

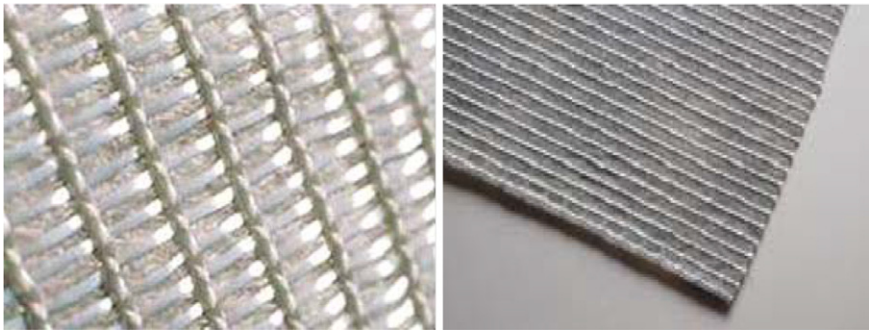

Figure 4. Geotextiles: (a) GT_{75} and GT_{95} (biaxial), (b) GT_{230} (uniaxial)

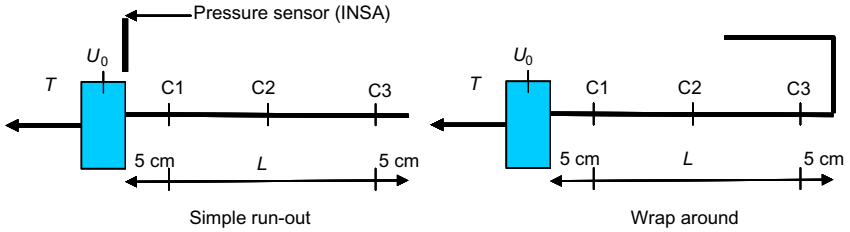

Figure 5. Displacement sensors position

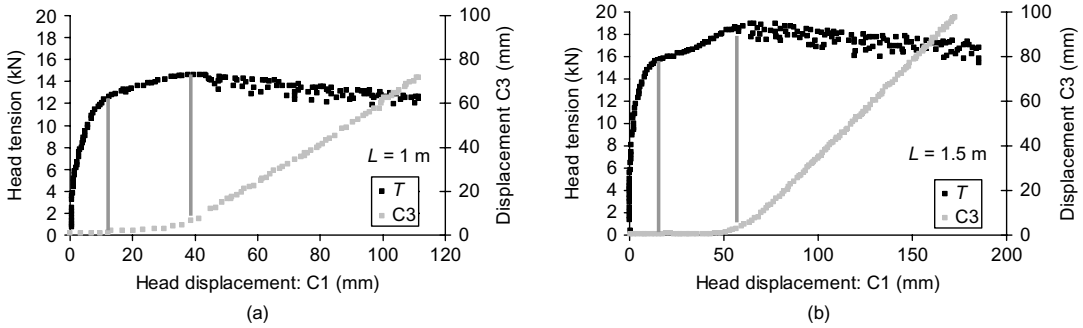

Figure 6. Comparison between the tension and the geosynthetic displacement (simple run-out ($b = 1$ m and $H = 0.4$ m) with the Irstea anchorage bench (GT95 and sand 2)): (a) $L = 1$ m; (b) $L = 1.5$ m

tensioning of the sheet, the curve after the second point corresponded to the pulling out of the sheet due to the fact that the point C3 was then moving at a constant rate. Between these two points, friction mechanisms combined with stretching of the sheet occurred in the vicinity of the geosynthetic/soil interface. Abutment mechanisms of the soil against the vertical wall of the anchorage bench were also observed.

The mechanisms appeared to be identical regardless of the anchorage length. The displacements were given based on C1 to eliminate the error of the displacement between the metallic clamp (U_0) and the beginning of the anchorage (C1).

Table 3 shows the values of the tension and the displacement in the simple run-out for different types of geotextiles, soil and different geometric parameters (L, b (anchorage width) and H). Parameters T_{C2} and T_{C3}, respectively, are the tensions reached when the middle and the end of the sheet move, and T_{max} is the maximum anchorage capacity.

The parameters U_{C2} and U_{C3} are the head displacement (C1) necessary when the point C2 and C3, respectively, started to move.

For the INSA bench, Figure 7 shows the different point displacements (C2 and C3) of the reinforcement and the head tension (T) plotted against the head displacement (C1) during the extraction for the two types of geotextile in the sand. Point C2 was at the middle of the reinforcement and point C3 was situated at 0.05 m from the rear of the reinforcement (Figure 5).

As can be seen, similar anchorage mechanisms to those obtained previously for the Irstea bench, were observed with two inflection points on the tension curve for the GT_{75} whereas, there was only one inflection point for the GT_{230} (Figure 7).

Important longitudinal displacements (around 80 mm) in the GT_{75} were observed at the end of the pull-out test (Figure 7). This led to an increase in length and a small reduction in the width of the reinforcement. This stretching of the geosynthetic had an influence on the interaction

Table 3. Results of simple run-out anchorage

Soil	GSY/J (kN/m)	L (m)	b (m)	H (m)	T_{C2} (kN/m)	T_{C3} (kN/m)	T_{max} (kN/m)	U_{C2} (mm)	U_{C3} (mm)
Sand 1	GT_{75} /687	1	0.5	0.4	6.2	10	11.2	6.7	62
	GT_{75} /687	1	0.5	0.5	8.8	16	16	8.3	96
Sandy silt	GT_{75} /687	2	1	0.36	12	14.2	14.2	18	72
Sand 2	GT_{95} /870	1	1	0.4		11.7	14.7		9.4
	GT_{95} /870	1.5	1	0.4		14.1	18.5		15.6
	GT_{95} /870	1.5	1	0.4		13	17		12.3
Sand 1	GT_{230} /2104	1	0.5	0.4	6.4	10.2	11.6	3.9	7.4
	GT_{230} /2104	1	0.5	0.5	10.8	14.6	16.8	5.7	8.7
Gravel	GT_{230} /2104	1	0.5	0.4	8	14.8	20	3.9	9.4
	GT_{230} /2104	1	0.5	0.5	7.4	16.4	28	2.5	7.4

L, anchorage length; b, anchorage width; GSY, geosynthetic; J, stiffness.

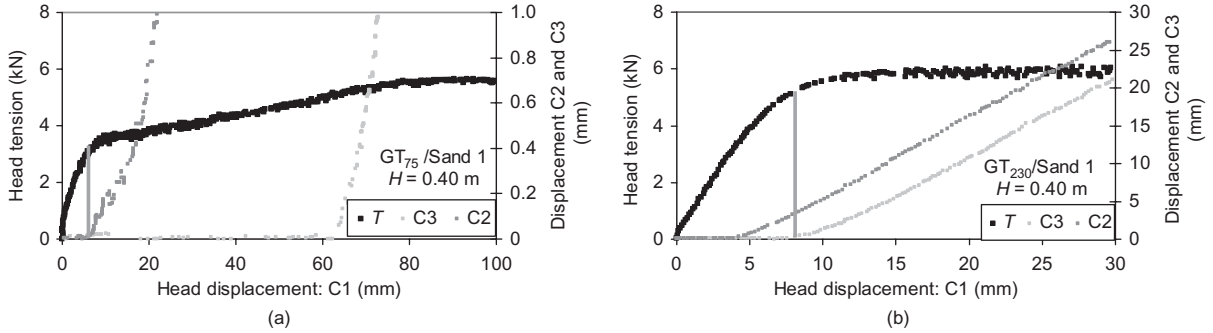

Figure 7. Comparison between the tension and the geosynthetic displacement (simple run-out ($L = 1$ m and $b = 0.50$ m) with the INSA anchorage bench and sand 1): (a) GT_{75}, (b) GT_{230}

between the soil and the geosynthetic, which could explain the second slope.

By comparison, in the case of GT_{230} (Lajevardi *et al.* 2014), the curve T–C1 may be assimilated to a bi-linear law (Figure 7b): Points C2 and C3, respectively, started to move when C1 was equal to 3.9 and 7.4 mm. Due to the strong stiffness, the stretching of the geosynthetic was not so important (the plateau was reached when the rear of the geotextile started to move; C1 was equal to 7.4 mm) and so gave a bi-linear law. Moreover, longitudinal displacements of the wires in the GT_{230} were observed at the end of the pull-out test (Figure 8). This could also disrupt the global pull-out behaviour.

It was concluded that for these two benches, two mechanisms were found.

- The first was for geosynthetic reinforcements with low stiffness values (GT_{75} and GT_{95}). For a flexible geosynthetic, regardless of the bench the same behaviour with two inflection points was observed in the curve of the graph of tension plotted against the head displacement.
- For the stiffer geosynthetic reinforcement (Figure 7b; GT_{230}), there was only one inflection point.

For simple run-out with the INSA anchorage bench, Figure 9 shows the curve of tension plotted against head displacement (T–C1) and the curve of horizontal stress plotted against head displacement (σ_h–C1) for GT_{230} in two types of soil. These curves with similar shapes show that there was an abutment effect above the metallic clamp whatever the soil. The soil was pushed towards the metallic clamp whereas the geosynthetic sheet was pulled out. Due to friction between the soil and the metallic clamp which disturbed the horizontal and vertical stress states locally, the real anchorage capacity could be increased by this abutment and the INSA anchorage bench overestimated the required tension to extract the geosynthetic.

3.2. Wrap around anchorage

Figure 10 shows the head tension and the rear displacement (C3) plotted against the head displacement (C1) of the geotextile for the wrap around anchorage in the Irstea anchorage bench. Tables 4 and 5 show the results of this anchorage system. For easier comparisons between the several tests, the tension unit is presented in kN/m in these tables.

Figure 10 and Tables 4 and 5 show that whatever the soil or the test apparatus, the same conclusion was obtained: there was an optimum length of the upper part of sheet (B) required to mobilise an abutment in the soil, equal or lower than the smaller one tested (0.25 m).

3.3. Anchorage capacity: comparison between two different anchorage systems

The tests were carried out on the geotextile sheets with the same length for their lower part (L) show that for the large head displacement, the anchorages with wrap around were

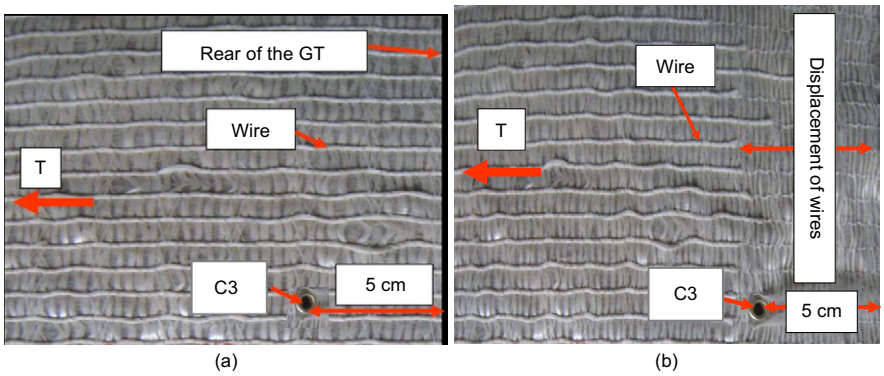

Figure 8. Longitudinal displacement of the reinforcement wires for GT_{230}: (a) before the test; (b) after the test

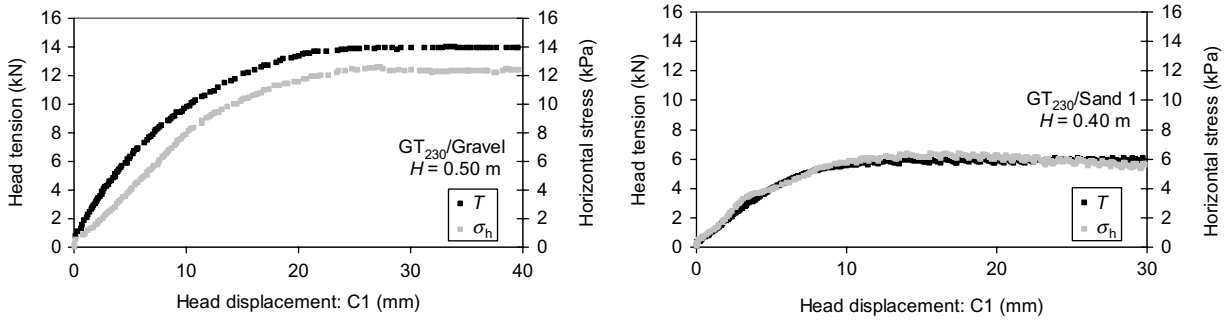

Figure 9. Simple run-out anchorage ($b = 0.50$ m): comparison between the tension (T) and the horizontal stress (σ_h) measured above the metallic clamp with a pressure sensor

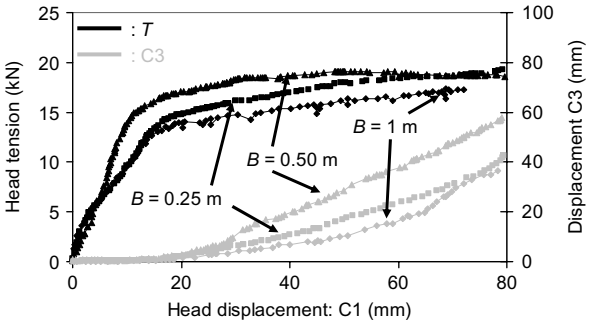

Figure 10. Anchorages with wrap around in the Irstea anchorage bench (GT_{95}, Sand 2, $b = 1$ m, $L = 1.5$ m)

more resistant than the simple run-out anchorage system (Tables 4 and 5 and the relationship T_{max_wa}/T_{max_sr}). They show an increase in the maximum tension of between 12 and 27%.

3.4 Influence of parameters on the tension

3.4.1 *Effect of B*

In the wrap around anchorage, the length variation of upper part of sheet (B) was not an important factor for the tension. Figure 11 and Tables 4 and 5 show two ($B = 0.25$ and 0.50 m at INSA) or three ($B = 0.25$, 0.50 and 1 m at Irstea) lengths of upper part of sheet, the first ($B = 0.25$ m) is largely sufficient.

The tension was not proportional to the length of the sheet upper part and the mechanisms induced by this length were not only friction but also included an abutment effect. It seems that a minimum length of the upper part of the sheet (B) was needed to mobilise an abutment effect in the soil and to increase the anchorage capacity.

3.4.2 *Effect of H and D_1*

The variations in the height of cover (H: in the simple run-out anchorage and D_1: in the wrap around anchorage, with $H = D_1 + D_2$ and D_2 was always 0.20 m) on the tension in the pull-out tests have an important influence. Table 6 shows that for the GT_{75} and GT_{230}, this influence was around 40%.

The experimental studies had the disadvantage of cost, time of design and construction (approximatively one test per week). They typically focused on the definition of new model parameters due to the use of new anchorage shapes or of new materials. Furthermore, they did not allow access to all the data in terms of stresses or strains in the structures. The use of a numerical model is then interesting. Numerical modelling allowed the stability, the deformation and the influence of various parameters in the model to be analysed.

In the present study, a specific two-dimensional DEM was used. Discontinuous approaches permitted the simulation of discrete particles interacting with each other, which was not the case for the classical continuum mechanical approach. This type of modelling permitted the limits of continuous modelling to be exceeded. The DEM depicted the soil and the geosynthetic as discrete

Table 4. Results of anchorages with wrap around inside sand 1 with the INSA bench ($b = 0.5$ m)

GSY	D_1 (m)	H (m)	B (m)	T_{max_wa}* (kN/m)	T_{max_sr}* (kN/m)	T_{max_wa}*/ T_{max_sr}*
GT_{75}	0.2	0.4	0.25	13	11.2	1.16
			0.5	14		1.25
	0.3	0.5	0.25	18.1	16	1.13
			0.5	19.4		1.21
GT_{230}	0.2	0.4	0.25	14.2	11.6	1.22
			0.5	14.8		1.27
	0.3	0.5	0.25	20.6	16.8	1.22
			0.5	21.2		1.26

*: wa: wrap around, sr: simple run-out.

Table 5. Results of wrap around anchorages inside gravel with the INSA bench ($b = 0.5$ m)

GSY	D_1 (m)	H (m)	B (m)	T_{max_wa}* (kN/m)	T_{max_sr}* (kN/m)	T_{max_wa}*/ T_{max_sr}*
GT_{75}	0.2	0.4	0.25	26.8	23.4	1.15
			0.5	27.2		1.16
GT_{230}	0.2	0.4	0.25	23.4	20	1.17
			0.5	23.4		1.17
	0.3	0.5	0.25	31.4	28	1.12
			0.5	33.8		1.21

*wa, wrap around; sr, simple run-out.

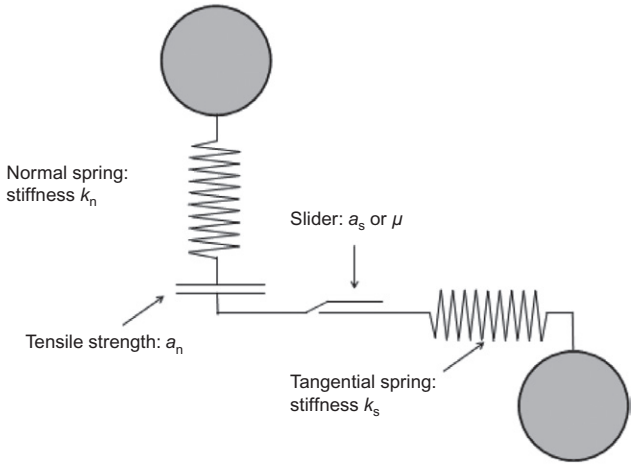

Figure 11. Interaction between two particles with DEM (Chareyre and Villard 2002)

elements which were connected. This method modelled the granular media by a set of independent elements with different sizes, interacting via their contact points. This principle of discrete simulation allowed the modelling of media with unlimited deformations and displacements and also macroscopic discontinuities within the model. The final state could be different from the initial state. The geometry changed significantly during calculation (especially in the soil/geosynthetic interface). For these reasons, this method seemed well suited to the simulation of the anchorage tests.

4. NUMERICAL MODEL

4.1. Discrete-element model

Numerical modelling was carried out with the DEM developed first by Cundall and Strack (1979). The DEM assumes a set of particles interacting with one another at points of contact (Figure 11), and can be used to simulate large relative displacements. This method is particularly well suited to the problem being considered here, since it provides the possibility to take into consideration the major movements and large-scale deformation of the soil (rotation, compression and lifting) as well as the large displacements between the geotextile and the soil (shear bands, crushing or overall rotation).

Interaction models, locally defined via micro-mechanical parameters of the contact models, make it possible to restore a global macroscopic behaviour of the particles assembly. This prevents direct introduction of constitutive models such as those defined by the mechanics of continuous media. A change of scale is required in order to obtain from the measurable geotechnical parameters (friction, cohesion) the parameters of the numerical model. A two-dimensional DEM, PFC2D (Itasca Consulting Group 1996), was used to investigate the pull-out behaviour of linear and non-linear geosynthetic anchorage. The geosynthetic sheet was modelled using the dynamic spar elements method (DSEM) proposed by Chareyre and Villard (2005), which were implemented into the DEM software. The thin spar elements (Figure 12) allowed the tensile behaviour of the geosynthetic sheet (no compression forces and no bending strength in the elements) to be reproduced using the tensile stiffness modulus parameter J (kN/m). The interface friction behaviour was governed by a Mohr–Coulomb law: $\tau_{max} = a_s + \sigma_n \tan \delta$, where a_s, δ and σ_n are the shear strength at a null normal stress (cohesion), the friction angle and the normal stress acting at the interface, respectively.

The soil was modelled with cylindrical particles, which were assembled together to make clusters. Each cluster was made of two jointed cylindrical particles of diameters d and $0.9d$. Clusters were used rather than single cylinders in order to reach high values of the macroscopic internal friction angle of the soil.

The granular distribution, initial porosity, shape of clusters and the methodology of setting up the particles had a great influence on the macroscopic behaviour.

For the present study, the cluster assembly was generated at a fixed porosity in a rectangular area without gravity, using the radius expansion with decrease of friction process (REDF) (Chareyre and Villard 2005). The elastic behaviour of the granular assembly depended on two local contact parameters: the normal stiffness k_n and shear stiffness k_s. For cylindrical particles, the normal and shear stiffness and strength were given by unit length. Two contact failure criteria were defined (Itasca Consulting Group 1996; PFC2D): one under tension, characterised by a tensile strength limit a_n, the other based on the elastic perfectly plastic model proposed by Cundall and Strack (1979) and characterised by shear strength a_s

Table 6. Influence of the parameters on the tension for sand 1 and gravel on GSY

Parameter	Definition	Domain investigation (m)	Anchorage	Soil	GSY*	Difference for T^*(%)
H	Thickness of soil layer above anchorage	0.40–0.50	Simple	Sand 1	GT_{75}	46
					GT_{230}	43
				Gravel	GT_{75}	#
					GT_{230}	38
D_1	Distance between upper and lower parts of GSY	0.20–0.30	Wrap around	Sand 1	GT_{75}	40
					GT_{230}	45
				Gravel	GT_{75}	#*
					GT_{230}	44

*GSY, geosynthetic; T, tension; #, the failure of the geotextile, the parameter 'difference for T' is calculated by reference to the smallest value of the Domain investigation. For example: $[(T_{H=0{\cdot}50\ m} - T_{H=0{\cdot}40\ m})/T_{H=0{\cdot}40\ m}]$ in %.

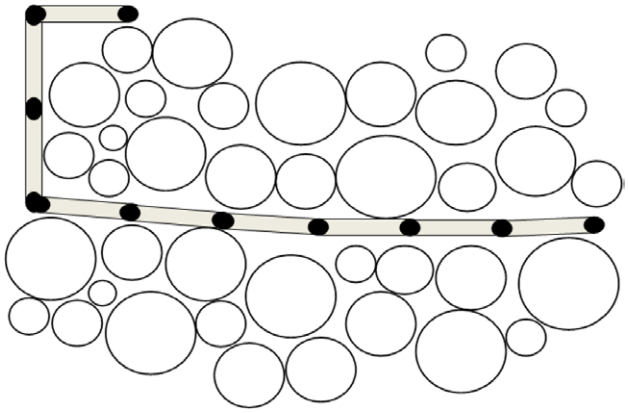

Figure 12. Spar element representation (Chareyre and Villard, 2005)

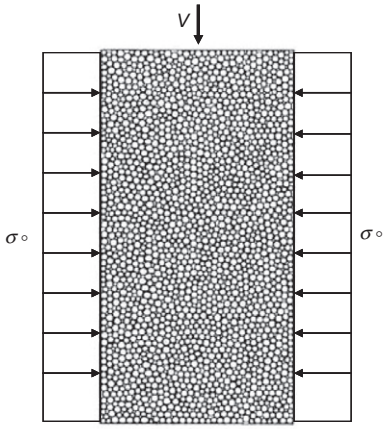

Figure 13. Geometry of the sample

(independent of normal force) or by a microscopic contact friction angle δ.

4.2. Macro-mechanical behaviour

The identification of the micro-mechanical contact parameters (Chareyre and Villard 2002) was obtained by reproducing and fitting the macro-mechanical behaviour of a sample of soil submitted to the usual laboratory tests. Numerical results of biaxial tests with around 4000 clusters are presented (Figure 13). Biaxial compression was simulated by imposing a translation speed V on the upper wall while the interlocked side walls maintained a constant lateral stress σ_0. The four walls were nonfrictional. The compression speed chosen was sufficiently slow to eliminate dynamic phenomena interference with the results. The strains and stresses were deduced directly from the displacement and the forces exerted on the walls.

As the modelling focus on the INSA bench pull-out tests on sand 1, triaxial tests on sand 1 were performed at LGCIE laboratory (INSA) with a constant confining stress σ_0 of 10, 20 and 50 kPa during the test procedure. A macroscopic friction angle φ' of 38.4° and an elastic modulus of 20 MPa were obtained.

Micro-mechanical parameters were chosen to fit this frictional macro-mechanical behaviour (Figure 14 and Table 7). Parameter k_n was related to the Young modulus, and the ratio k_s/k_n was related to the Poisson coefficient; k_n was obtained to fit the tangent elastic modulus and a ratio of $k_s/k_n = 0.5$ was chosen for this study. As the tests were performed on sand there was no tensile strength a_n and no shear strength a_s at a null normal stress. The inter-particle friction angle δ was calibrated with the peak value of the triaxial curve, and the porosity was obtained with the ratio of the friction angle at the peak over the residual friction angle.

The micro-mechanical parameters obtained are summarised in Table 7.

4.3. Numerical pull-out tests

Numerical pull-out tests were performed using between 25 000 and 40 000 clusters (width of 0.5 m) of several sizes. The displacement boundary conditions were imposed using rigid walls on the left, the right and on the bottom of the numerical sample. The extraction of the geosynthetic was carried out by moving the first sheet element horizontally. The dimensions of the experimental model were used in the modelling. The model is presented in Figure 15 for simple run-out and wrap around anchorages.

Due to the random character of the initial granular assembly, two successive simulations of the same problem never give exactly the same result. Thus, each numerical simulation was therefore performed three times to obtain average curves and values (Briançon *et al.* 2008).

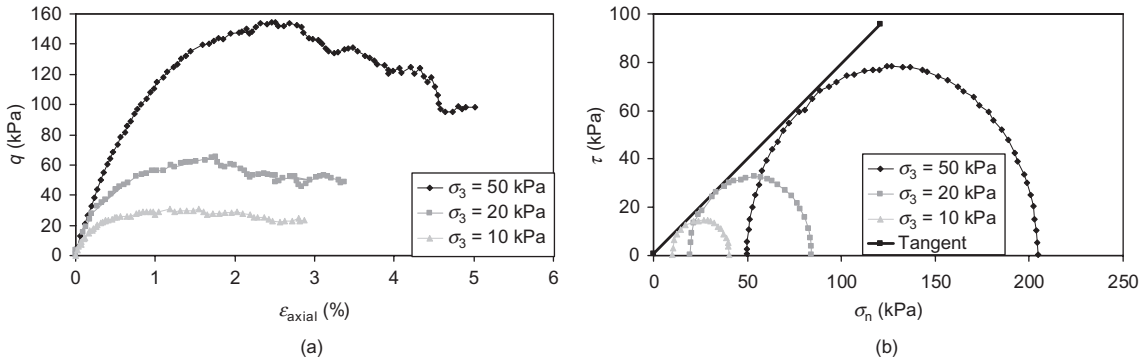

Figure 14. Numerical results of biaxial tests (a) and equivalent Mohr circles at failure (b). q, stress deviator; ε_{axial}, axial strain; τ and σ_n, shear and normal stresses

Table 7. Micro-mechanical parameters obtained by reproducing the macro-mechanical behaviour of sand 1

Soil modelling properties	Value
Micro-mechanical parameters	
Tensile stiffness k_n (kN/m²)	7×10^4
Shear stiffness k_s (kN/m²)	3.5×10^4
Inter-particle friction angle δ (°)	31
Shear strength a_s (N/m)	0
Tensile strength a_n (N/m)	0
Porosity	0.2

Figure 16 shows the comparison between three tests performed with three different initial grain generations. It demonstrates the good repeatability of simulations in which the maximum head tension value was reproduced. In the following tests, each numerical curve is taken as an average of three tests performed with three different initial grain generation.

The numerical tests were only focused on the INSA anchorage bench on GT_{230} ($B = 0.5$ m, Tables 3 and 4) for simple run-out and wrap around anchorages in sand 1 (cohesion $a_s = 0$).

Micro-mechanical parameters for the soils were used in these simulations. The parameter used for the geosynthetic sheet (tensile rigidity: J) was the one given in Table 2 (data from the geosynthetic manufacturer). The numerical interface friction angle between soil and the geosynthetic sheet (Mohr–Coulomb model) was calibrated from an experimental test performed on a simple run-out with a 0.40 m thick soil layer above the anchorage (H). This angle value was kept constant for all the simulations ($\varphi_{soil/geosynthetic} = 25.6°$). The friction between the wall and clusters was set to $\varphi_{soil/wall} = 28°$, as measured in the experimental tests.

Figure 17 shows the calibration from pull-out tests on the GT_{230} simple run-out anchorage with 0.40 m of thickness of soil layer above anchorage (H), and the comparison between numerical and experimental (INSA) results with a thicker soil layer above the anchorage ($H = 0.50$ m). The numerical curves have the same shape as the experimental curves: a first slope that corresponds to the tensioning and the plateau of the geosynthetic sheet. The experimental and numerical curves with $H = 0.50$ m of soil agreed well for the plateau value. In the tensioning part, the numerical curves were steeper, the tensile rigidity: J was calculated using the tensile tests without any confining. This means that the tensile rigidity changed as the soil below and above anchorage changed. Nevertheless, the head displacements for the plateau for both curves were quite similar and so the following simulations were performed with the former tensile rigidity J.

Figure 18 shows pull-out tests on a geosynthetic sheet with wrap around on GT_{230} with $B = 0.25$ or 0.50 m of return and 0.40 m thickness of the soil layer above the anchorage (0.20 m below (D_1) and 0.20 m above (D_2) return). The curves still represent the head tension function of the head displacement and the general tendency was reproduced. For the calibration of the soil/geosynthetic interface friction on simple run-out anchorage, the numerical curves overestimated the experimental ones with a maximum difference of 8%. The numerical curves also show that between $B = 0.25$ and 0.50 m, the contribution of return was negligible.

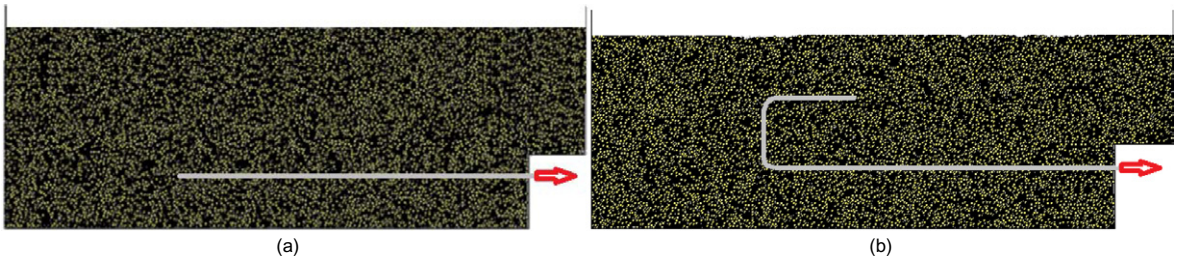

Figure 15. Numerical modelling of INSApull-out test: (a) simple run-out, (b) wrap around

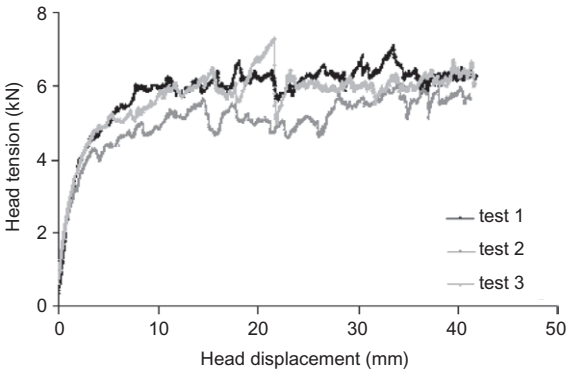

Figure 16. Comparison between three numerical tests performed with three different initial grain generation (INSA bench, $L = 1$ m, $H = 0.40$ m)

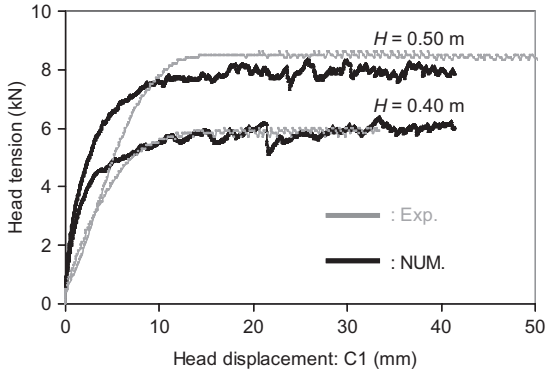

Figure 17. Comparison for Sand 1 between numerical and experimental pull-out tests (INSA simple run-out, width $b = 50$ cm) for $H = 0.40$ and 0.50 m thickness of soil layer above anchorage (calibration done with $L = 1$ m, $H = 0.40$ m)

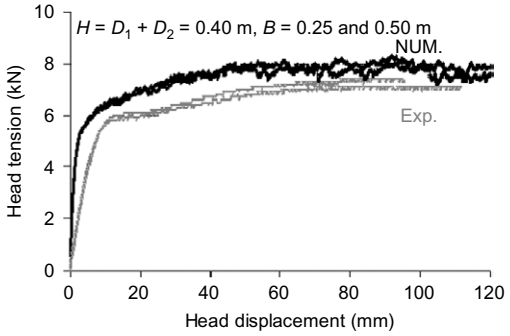

Figure 18. Comparison for Sand 1 between numerical and experimental (INSA, width $b = 50$ cm) pull-out tests on GT_{230} with wrap around for $H = 0.40$ m ($D_1 = D_2 = 0.20$ m) for upper part of sheet $B = 0.25$ and 0.50 m

Table 8. Influence of the upper part of sheet on GT_{230} with wrap around for $H = 0.40$ m ($D_1 = D_2 = 0.20$ m) for $B = 0.125$, 0.25, 0.50 and 0.75 m

B (m)	T_{max} (kN)	$T_{max}/T_{max(B = 0{\cdot}125\ m)}$
0.125	7.9	1
0.25	8.2	1.04
0.50	8.35	1.06
0.75	8.5	1.08

These first simulations showed that the numerical discrete model was well able to reproduce the experimental pull-out tests.

Additional simulations (Table 8) were performed to evaluate the influence of the length of return $B = 0.125$, 0.25, 0.50 and 0.75 m. The influence of the length of the upper part of the sheet was not significant (8%), which confirmed the experimental results in which there was an optimum length of the upper part of the sheet (B) required to mobilise an abutment in the soil.

Figure 19 shows the pull-out tests on geosynthetic sheet with wrap around on GT_{230} with 0.25 or 0.50 m of return and 0.50 m of thickness of soil layer above anchorage (0.30 m below (D_1) and 0.20 m above (D_2) return). Both curves fit nearly perfectly, showing that the calibration of the soil/geosynthetic interface friction from simple run-out anchorage results was adequate for wrap-around anchorage with different thicknesses of soil above.

Figure 20 presents the simulated and experimental head tensions for the geosynthetic sheet for both simple run-out and wrap around with $B = 0.25$ m. The anchorage capacity was more quickly mobilised for the simple run-out case. Moreover, the experimental tests (Table 4 and Figure 20)

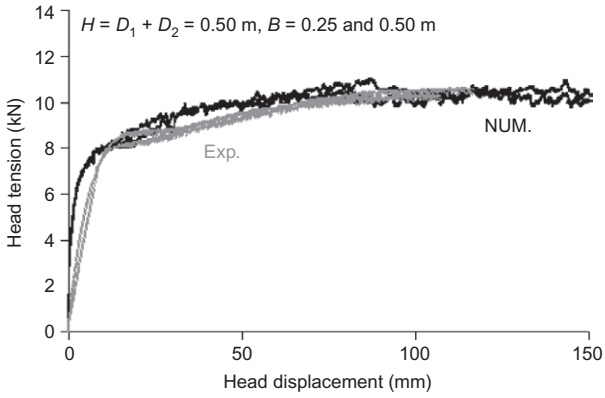

Figure 19. Comparison for Sand 1 between numerical and experimental (INSA, width $b = 50$ cm) pull-out tests on GT_{230} with wrap around for $H = 0.50$ m ($D_1 = 0.30$ m, $D_2 = 0.20$ m) for the upper part of sheet $B = 0.25$ and 0.50 m

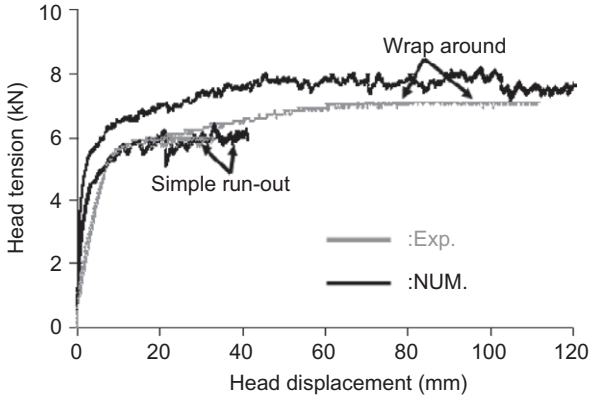

Figure 20. Comparison for Sand 1, $b = 0.50$ m between numerical and experimental (INSA, width $b = 50$ cm) pull-out tests on GT_{230} with simple run-out ($L = 1$ m) and wrap around for $H = 0.40$ m ($D_1 = D_2 = 0.20$ m) for upper part of sheet $B = 0.25$ m

have shown the contribution of wrap around in comparison with the simple run-out: wrap around led to an increase of 22% in the maximum head tension. The numerical tests showed the same tendency (Figure 20) with an increase of 30% of the maximum tensile strength.

4.4. Analysis at the micro-mechanical scale

The numerical modelling allows access to the stress–strain behaviour of the pull-out tests and provides a better understanding of what happens inside the soil mass using a fine analysis of some numerical outputs, at the micro-mechanical scale. For that purpose, a pull-out test with wrap around anchorage ($H = 0.40$ m, $B = 0.25$ m) was studied. Figure 21 presents the velocity vectors (between the initial state and the final state) of the particles obtained in a representative simulation.

Maximum velocities were observed along the horizontal part of the anchorage as it slides into the return of the anchorage which deformed during the test. Large displacements were also noticed behind the anchorage and above the upper part of the sheet where particles tended to move below as the wrap around distorted. Uplift was also observed on the top of sand 1 and at the right side above the wrap around, as the soil moved in the direction of tension. Experimental tests on sand 1 in which heave of the soil was measured, confirm the numerical results qualitatively (Figure 22). Nevertheless, it is important to note significant differences in terms of vertical displacements. Numerical modelling can only reproduce the phenomena qualitatively and overestimated the vertical movements (heave or settlement). This was probably due to the fact that the discrete element model did not reproduce the granulometry of the material and the fact that the discrete elements calculations were not of three-dimensional shapes like the soil particles.

4.5. Contact forces into the anchorage bench

Discrete element modelling enables contact force networks between soil particles to be noted. It makes it possible to observe the force diffusion and detect possible particle destabilisation during numerical tests. Figures 23 and 24 show the distribution and evolution of the contact forces (only tangential for clarity) on the bench during the pull-out tests for the simple run-out and wrap around anchorages, respectively. Each contact force is illustrated by a line connecting the centres of two particles. The width of the line is proportional to the magnitude of the contact force.

Initially, contact forces were stronger in the lower part of the tank due to the gravity (Figure 23a). During the tensioning of the geosynthetic sheet contact forces densified near the front face of the box and close to the soil/geosynthetic interface and rotations occurred in the horizontal extraction direction (Figure 23b): the load was transferred from the geosynthetic sheet to the sand by frictional resistance which caused changes in the contact force distribution and orientation, as observed by Wang *et al.* in geogrid numerical modelling (Wang *et al.* 2014).

The contact forces network was also explored in the wrap around anchorage (Figure 24) for two different displacements during extraction. The phenomenon of reorientation of the forces towards the tension direction was also observed in the wrap around anchorage case. Other phenomena were observed because of the shape of the anchorage: contact forces tended to densify into the anchorage return (Figure 24a) under its deformation during extraction. Soil was confined, leading to an abutment of soil mass. Other force chain concentrations can be observed above the anchor block: the soil was pushed towards the vertical wall during the geotextile tension, leading to soil abutment of the upper part of the bench (Figure 24b).

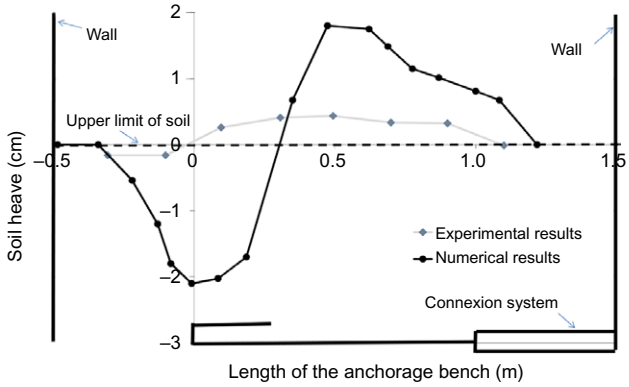

Figure 22. Heave of the soil (Sand 1, GT_{230}, $B = 0.25$ m, $H = 0.40$ m)

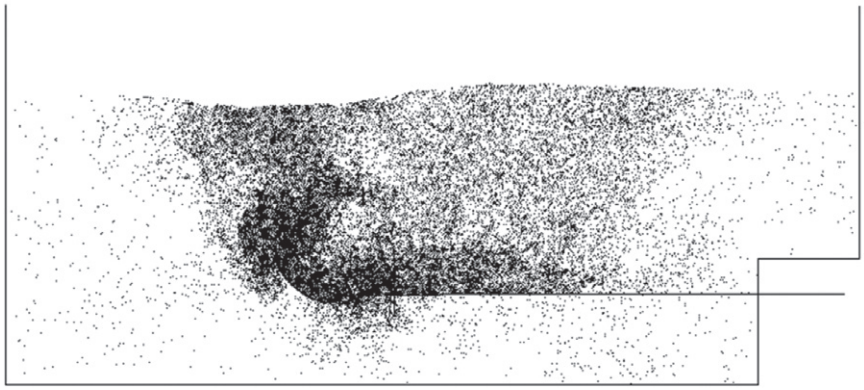

Figure 21. Two-dimensional velocity field during a pull-out test on wrap around anchorage ($B = 0.25$ m, $H = 0.40$ m)

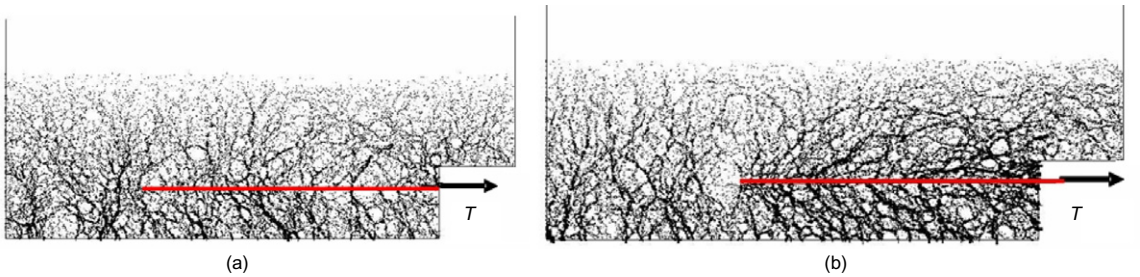

Figure 23. Force contact network in the bench (simple run-out: GT_{230} with $H = 0.40$ m): (a) before test, (b) after test

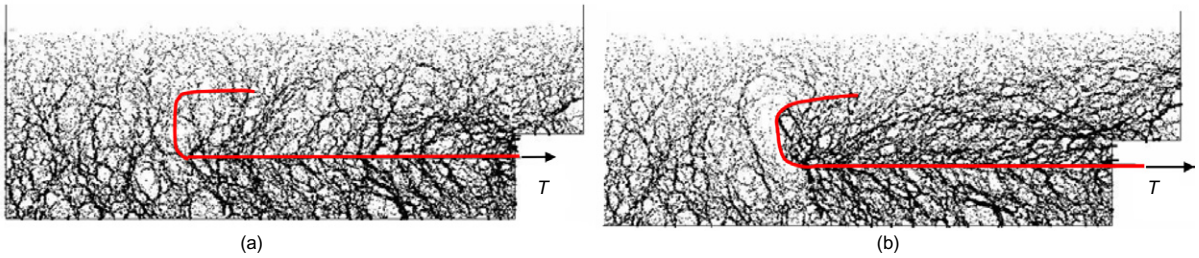

Figure 24. Contact force distribution in the bench during pull-out tests with wrap around for two different head displacements: C_1 (6 and 60 mm) and $H = 0.40$ m, $B = 0.25$ m): (a) 6 mm, (b) 60 mm

On the contrary, the contact forces network was not very dense behind the wrap around anchorage. Particles in this area were destabilised and did not participate any more to the force transmission into the bench.

Finally, the contact forces gradually concentrated more and more in the right part of the tank, as the geosynthetic sheet was being pulled towards the right direction. As a result, with both the simple run-out and the wrap around anchorage the contact forces tended globally to orientate diagonally as they initiated from the vertical wall above the anchor block and moved towards the horizontal part of the geosynthetic sheet and down to the lower part of the tank, as observed by Tran *et al.* (2013) and Wang *et al.* (2014).

5. CONCLUSION

Experimental pull-out tests were performed with two types of anchorage benches (Irstea, INSA Lyon) under laboratory-controlled conditions with three types of geotextiles (uniaxial or biaxial with different stiffness) and in the presence of cohesive and non-cohesive soils for the simple run-out and the wrap around anchorages.

The results show that the behaviour of the geotextile sheet on the two types of anchorage benches was very similar. These tests allowed the influence of various parameters on the geotextile behaviour: anchorage capacity, length of the upper part of the sheet (B), soil type and geotextile type to be investigated.

In order to complete the experimental studies, a specific two-dimensional numerical model was used. The results of the experimental tests provide an interesting database to be created on which numerical calculations can be validated. Experimental tests performed with the INSA anchorage apparatus were simulated with a DEM.

Numerical pull-out tests were performed for the simple run-out and the wrap around anchorages in the anchorage bench with sand. The numerical model chosen gave a good representation of the phenomena that were observed in the experiments (abutment, uplift).

The results of the numerical model for the simple run-out and the wrap around anchorages (head tension versus head displacement) in the tests with sand shows that the selected numerical method fitted relatively well with the experimental anchorage tests (with a maximum difference of 8%), thus validating the strength of this model to estimate anchorage capacities. In addition, the distribution of contact forces and displacements along the geosynthetic sheet at different clamp displacements showed the load transfer behaviour between the geosynthetic and the soil by frictional resistance, giving more insights at a microscopic scale.

The capacity of the geosynthetic sheet in traction increased from the simple run-out to the wrap around anchorage.

The influence of the length of the upper part of the geotextile sheet (B) was studied and it was found not to be significant (less than 8% for B ranging from 0.125 to 0.75 m). This confirmed the experimental results where there was an optimum length of the upper part of the sheet required to mobilise an abutment in the soil. Thus, a minimum length can be chosen to minimise costs on the site.

NOTATION

Basic SI units are given in parentheses.

a_s shear strength at a null normal stress (N/m)
a_n tensile strength at a null normal stress (N/m)
B length of the upper part of the sheet (m)

B width of the geosynthetic sheet or anchorage width (m)
c' cohesion (Pa)
C_1 head displacement of the geosynthetic sheet (m)
C_3 rear displacement of the geosynthetic sheet (m)
d diameter of cylindrical particles (m)
D_1 distance between the upper and the lower part of the geotextile (m)
D_2 distance between the upper part of the geosynthetic and the upper limit of the soil (m)
D_{10} soil particle diameter corresponding to 10% by weight of finer particles (m)
D_{30} soil particle diameter corresponding to 30% by weight of finer particles (m)
D_{60} soil particle diameter corresponding to 60% by weight of finer particles (m)
E elastic modulus (Pa)
H thickness of the soil layer above the anchorage (m)
J geotextile stiffness (N/m)
k_n tensile or normal stiffness (N/m^2)
k_s shear stiffness (N/m^2)
L length of the geotextile or anchorage (m)
T head tension (N)
T_{C2} tension reached when the middle of the sheet move (N/m)
T_{C3} tension reached when the end of the sheet move (N/m)
T_{max} maximum tension or maximum anchorage capacity (N/m)
T_{max_wa} maximum anchorage capacity for the wrap around (N/m)
T_{max_sr} maximum anchorage capacity for the simple run-out (N/m)
U_0 displacement of the metallic clamp (m)
U_{C2} necessary head displacement (C_1) when the point C_2 starts to move (m)
U_{C3} necessary head displacement (C_1) when the point C_3 starts to move (m)
V translation speed on the upper wall (m/s)
w water content (dimensionlesss)
γ_d dry unit weight(N/m^3)
δ interparticle friction angle (degrees)
ε_{axial} axial strain (dimensionless)
σ_h horizontal stress (Pa)
σ_0 constant lateral stress or constant confining stress (Pa)
σ_n normal stress acting at the interface (N/m^2)
σ_n normal stress (Pa)
φ' friction angle (degrees)
$\varphi_{soil/geosynthetic}$ friction between geosynthetic and clusters (degrees)
$\varphi_{soil/wall}$ friction between wall and clusters (degrees)
τ shear stress (Pa)
τ_{max} maximum shear stress (N/m^2)

REFERENCES

Abdelouhab, A., Dias, D. & Freitag, N. (2010). Physical and analytical modelling of geosynthetic strip pull-out behaviour. *Geotextiles and Geomembranes* **28**, No. 1, 44–53.

Alfaro, M. C., Miura, N. & Bergado, D. T. (1995). Soil geogrid reinforcement interaction by pullout and direct shear tests. *Geotechnical Testing Journal*, **18**, No. 2, 157–167.

ASTM D6706-01 *Standard Test Method for Measuring Geosynthetic Pullout Resistance in Soil*. ASTM International, West Conshohoken, PA, USA.

Bhandari, A. & Han, J. (2010). Investigation of geotextile–soil interaction under a cyclic vertical load using the discrete element method. *Geotextiles and Geomembranes*, **28**, No. 1, 33–43.

Briançon, L., Girard, H. & Villard, P. (2008). Geosynthetics anchorage: experimental and numerical studies. *Proceedings of EuroGeo4 – the 4th European Geosynthetics Conference*, Edinburgh.

BSI (2004). *BS EN 13738:2004: Geotextiles and Geotextile-related Products. Determination of Pullout Resistance in Soil*. BSI, London, UK.

Calvarano, L. S., Cardile, G., Gioffrè, D. & Moraci, N. (2013). Experimental and theoretical study on interference phenomena between the bearing members of different geogrids in pullout loading conditions. *Proceedings of Geosynthetics 2013*, Long Beach, Paper no.78, pp. 496–502.

Cazzuffi, D., Moraci, N., Calvarano, L. S., Cardile, G., Gioffrè, D. & Recalcati, P. (2014). European experience in pullout tests: Part 2 – The influence of vertical effective stress and of geogrid length on interface behaviour under pullout conditions. *Geosynthetics*, **32**, No. 2, 40–50.

Chareyre, B. & Villard, P. (2002). Discrete element modelling of curved geosynthetic anchorages with known macro-properties. *Proceedings of the First International PFC Symposium*, Gelsenkirchen, Germany, 6–7 November, Konietzky, H. (ed), Swets and Zeitlinger, Lisse, the Netherlands, pp. 197–203.

Chareyre, B. & Villard, P. (2005). Dynamic spar elements and DEM in two dimensions for the modelling of soil-inclusion problems. *Journal of Engineering Mechanics – ASCE*, **131**, No. 7, 689–698.

Chareyre, B., Briançon, L. & Villard, P. (2002). Numerical versus experimental modelling of the anchorage capacity of geotextiles in trenches. *Geosynthetics International*, **9**, No. 2, 97–123.

Chen, C., McDowell, G. R. & Thom, N. H. (2012). Discrete element modelling of cyclic loads of geogrid-reinforced ballast under confined and unconfined conditions. *Geotextiles and Geomembranes*, **35**, 76–86.

Cundall, P. A. & Strack, O. D. L. (1979). A discrete numerical model for granular assemblies. *Geotechnique*, **29**, No. 1, 47–65.

De, A. & Vellone, D. A. (2005). Experimental and numerical modeling of 248 geosynthetic anchor trench. *Geo-Frontiers 2005 Congress*, Austin, TX, USA.

Ferellec, J. F. & McDowell, G. R. (2012). Modelling of ballast–geogrid interaction using the discrete-element method. *Geosynthetics International*, **19**, No. 6, 470–479.

Girard, H., Briançon, L. & Rey, E. (2006). Experimental tests for geosynthetic anchorage trenches. *Proceedings of the Eighth International Conference on Geosynthetics, 8th ICG*, Yokohama, Japan, 18–22 September 2006, pp. 211–216.

Gourc, J. P., Reyes-Ramirez, R. & Villard, P. (2004) Assessment of geosynthetics interface friction for slope barriers of landfill. *Proceedings of GeoAsia Conference*, Seoul, Korea, June 2004, pp. 116–149.

Han, J., Bhandari, A. & Wang, F. (2012). DEM analysis of stresses and deformations of geogrid-reinforced embankments over piles. *International Journal of Geomechanics*, **12**, No. 4, 340–350.

Itasca Consulting Group (1996) *Particles Flow Code in Two Dimensions: PFC2D User's Manual*, version 1.1. Itasca, Minneapolis, MN, USA.

Khedkar, M. S. & Mandal, J. N. (2009). Pullout behaviour of cellular reinforcements. *Geotextiles and Geomembranes*, **27**, No. 4, 262–271.

Lajevardi, S. H., Dias, D. & Racinais, J. (2013). Analysis of soil-welded steel mesh reinforcement interface interaction by pull-out tests. *Geotextiles and Geomembranes*, **40**, No. 2013, 48–57.

Lajevardi, S. H., Briançon, L. & Dias, D. (2014). Experimental studies of the geosynthetic anchorage – Effect of geometric parameters and efficiency of anchorages. *Geotextiles and Geomembranes* **42**, No. 5, 505–514.

Lajevardi, S. H., Briançon, L. & Dias, D. (2015). Experimental studies of the behaviour of geosynthetic wrap around anchorage. *Geosynthetics International*, **22**, No. 3, 249–256.

Lin, Y. L., Zhang, M. X., Javadi, A. A., Lu, Y. & Zhang, S. L. (2013). Experimental and DEM simulation of sandy soil reinforced with H–V inclusions in plane strain tests. *Geosynthetics International*, **20**, No. 3, 162–173.

Moraci, N. & Recalcati, P. G. (2006). Factors affecting the pullout behaviour of extruded geogrids embedded in compacted granular soil. *Geotextiles and Geomembranes*, **24**, No. 22, 220–242.

Moraci, N., Cardile, G., Gioffrè, D., Mandaglio, M.C., Calvarano, L.S. & Carbone, L. (2014). Soil geosynthetic interaction: design parameters from experimental and theoretical analysis. *Transportation Infrastructure Geotechnology*, **1**, No. 2, 165–227.

McDowell, G. R., Herireche, O., Konietzky, H. & Brown, S. F. (2006). Discrete element modelling of geogrids reinforced aggregates. *Proceedings of the Institution of Civil Engineers – Geotechnical Engineering*, **159**, No. 1, 35–48.

Palmeira, E. M. (2009). Soil-geosynthetic interaction: modelling and analysis. *Geotextiles and Geomembranes*, **27**, No. 5, 368–390.

Sieira, A. C. C. F., Gerscovich, D. & Sayao, A. S. F. J. (2009). Displacement and load transfer mechanisms of geogrids under pullout condition. *Geotextiles and Geomembranes*, **27**, No. 4, 241–253.

Stahl, M., Konietzky, H., te Kamp, L. & Jas, H. (2014) Discrete element simulation of geogrid-stabilised soil. *Acta Geotechnica*, **9**, No. 6, 1073–1084.

Su, L. J., Chan, T. C. F., Yin, J. H., Shiu, Y. K. & Chiu, S. L. (2008). Influence of overburden pressure on soil nail pullout: resistance in a compacted fill. *Journal of Geotechnical & Geoenvironmental Engineering*, **134**, No. 9, 1339–1347.

Tran, V. D. H., Meguid, M. A. & Chouinard, L. E. (2013). A finite–discrete element framework for the 3D modeling of geogrid–soil interaction under pullout loading conditions. *Geotextiles and Geomembranes*, **37**, 1–9.

Villard, P., Chevalier, B., Hello, B. L. & Combe, G. (2009). Coupling between finite and discrete element methods for the modelling of earth structures reinforced by geosynthetic. *Computers and Geotechnics*, **36**, No. 5, 709–717.

Villard, P. & Chareyre, B. (2004). Design methods for geosynthetic anchor trenches on the basis of true scale experiments and discrete element modelling. *Canadian Geotechnical Journal*, **41**, No. 6, 1193–1205.

Wang, Z., Jacobs, F. & Ziegler, M. (2014). Visualization of load transfer behaviour between geogrid and sand using PFC2D. *Geotextiles and Geomembranes*, **42**, No. 2, 83–90.

Zhang, J., Yasufuku, N. & Ochiai, H. (2007). A few considerations of pullout test characteristics of geogrid reinforced sand using DEM analysis. *Jioshinsetikkusu Rombunshu/Geosynthetics Engineering Journal*, **22**, 103–110.

Zhang, M. X., Qiu, C. C., Javadi, A. A., Lu, Y. & Zhang, S. L. (2013). Discrete-element method simulation of a model test of an embankment reinforced with horizontal–vertical inclusions. *Geosynthetics International*, **20**, No. 4, 238–251.

The Editor welcomes discussion on all papers published in Geosynthetics International. Please email your contribution to discussion@geosynthetics-international.com by 15 February 2016.